HHS Public Access

Author manuscript

Biol Psychiatry. Author manuscript; available in PMC 2021 June 01.

Published in final edited form as:

Biol Psychiatry. 2018 December 15; 84(12): 893–904. doi:10.1016/j.biopsych.2018.04.019.

Cocaine induced structural plasticity in input regions to distinct cell types in nucleus accumbens

Cindy Barrientos[#],
Neurobiology Section in the Division of Biological Sciences, University of California, San Diego, La Jolla, California

Daniel Knowland[#],
Neurosciences Graduate Program, University of California, San Diego, La Jolla, California, California

Mingche MJ Wu,
Neurobiology Section in the Division of Biological Sciences, University of California, San Diego, La Jolla

Varoth Lilascharoen,
Neurobiology Section in the Division of Biological Sciences, University of California, San Diego, La Jolla, California

Kee Wui Huang,
Nancy Pritzker Laboratory in the Department of Psychiatry and Behavioral Sciences at Stanford University School of Medicine, Palo Alto, California

Robert C. Malenka,
Nancy Pritzker Laboratory in the Department of Psychiatry and Behavioral Sciences at Stanford University School of Medicine, Palo Alto, California

Byung Kook Lim
Neurobiology Section in the Division of Biological Sciences, University of California, San Diego, La Jolla, California

[#] These authors contributed equally to this work.

Abstract

Background: The nucleus accumbens (NAc) is an extensively studied brain region implicated in pathological motivated behaviors such as drug addiction and is comprised predominantly of two discrete populations of neurons, dopamine receptor-1 and dopamine receptor-2 expressing medium spiny neurons (D1-MSNs and D2-MSNs, respectively). It is unclear whether these populations receive inputs from different brain areas and whether input regions to these cell-types undergo distinct structural adaptations in response to administration of addictive drugs such as cocaine.

Address correspondence to Byung Kook Lim, Ph.D., Department of Biological Sciences, University of California, San Diego, 9500 Gilman Dr. La Jolla, CA 92093; bklim@ucsd.edu.

Disclosures

The authors report no biomedical financial interests or potential conflicts of interest.

Methods: Using a modified rabies virus-mediated tracing method, we present a comprehensive brain-wide monosynaptic input map to D1- and D2-MSNs in the NAc. Next, we analyze nearly 2,000 dendrites and over 125,000 spines of neurons across four separate input brain regions (prelimbic cortex (PrL), medial orbitofrontal cortex (MO), basolateral amygdala (BLA), and ventral hippocampus (vHPC)) at four separate time points during cocaine administration and withdrawal to examine changes in spine density in response to cocaine.

Results: D1- and D2-MSNs display overall similar input profiles, with the exception that D1-MSNs receive significantly more input from the MO. We find that neurons in distinct brain areas (PrL, MO, BLA, and vHPC) projecting to D1- and D2-MSNs display different adaptations in dendritic spine density changes during different stages of cocaine administration and withdrawal.

Conclusions: While NAc D1- and D2-MSNs receive input from generally similar brain structures, spine density changes in specific input regions in response to cocaine administration are quite distinct and dynamic. While many previous studies have focused on input-specific postsynaptic changes in NAc MSNs in response to cocaine use, these findings emphasize the dramatic changes that also can occur in the afferent input regions as well.

Introduction

The nucleus accumbens (NAc) is a brain region critical for processing motivationally salient information from the environment and is one of the first brain areas to robustly respond to drugs of abuse (1–5). Indeed, animals will work to electrically self-stimulate the NAc to the exclusion of basic needs such as water and food (6). In addition to responding to rewarding stimuli, the NAc also plays a role in mediating aversive states (7). These seemingly opposite functions may arise in part because of the cellular diversity of the NAc. D1-MSNs and D2-MSNs represent largely non-overlapping NAc cell populations and comprise ~95% of all neurons in the region (8). Indeed, optogenetic manipulations suggest that D1-MSN stimulation is rewarding, while D2-MSN stimulation is aversive (9). Furthermore, D1-MSNs and D2-MSNs undergo distinct synaptic adaptations in response to cocaine administration (1, 2, 5, 10–13), possibly reflecting their different functional roles.

In addition to these cell-type specific differences, the NAc also receives brain-wide input from many different regions. The dense innervation of the NAc by ventral tegmental area dopaminergic neurons is thought to be critically important for the response to rewarding stimuli, in particular drugs of abuse (14). However, with the advent of optogenetics, recent research has uncovered critical roles for glutamatergic inputs from various areas of the brain including but not limited to the medial prefrontal cortex (mPFC), basolateral amygdala (BLA), and ventral hippocampus (vHPC)(1, 2, 15). Indeed, these excitatory afferents to the NAc have been suggested to underlie separate components of addictive behavior with the vHPC encoding contextual information, the BLA relaying emotional context, and the mPFC providing operational value (15).

While the mPFC, vHPC, and BLA are the most heavily studied NAc afferents, recent reports have underscored the importance of the paraventricular nucleus of the thalamus (PVT) and its synaptic connections with D2-MSNs during protracted drug use (12, 16). Thus, consideration of both cell type- and input-specific plasticity within the NAc is necessary to

fully capture the mechanistic complexity underlying drug-induced neural adaptations. Furthermore, a single exposure to an addictive drug normally induces relatively transient changes in neuronal function and normally does not lead to repeated use. Repeated exposure, however, induces stable and lasting changes in neural circuit function, which contribute to the maintenance of drug use and relapse during abstinences, due to cravings lasting for months or even years (17).

Drug-induced structural changes in neurons may play a particularly important role in mediating the long-lasting behavioral adaptations caused by repetitive administration of drugs of abuse (5). For example, increased spine density, a structural correlate of synaptic plasticity, and Delta-FosB expression after chronic cocaine treatment is stably maintained during long periods of withdrawal in D1-MSNs, but not in D2-MSNs (5, 11). Additionally, BLA inputs to D1-MSNs, but not vHPC inputs, exhibit an increase in both spine density and excitatory synaptic strength after repeated cocaine exposure (10). While spine changes have been thoroughly described in NAc MSNs, much less is known about whether similar cocaine-induced changes extend to the input structures themselves. Do cells projecting to NAc in input regions such as the mPFC, BLA, and vHPC exhibit spine density changes that parallel those observed in the NAc itself? Might such changes lie upstream of aberrant alterations in the NAc over the course of cocaine administration?

To begin to address these questions, we first provide a brain-wide characterization of all inputs to NAc D1- and D2-MSNs using viral-mediated monosynaptic circuit tracing in appropriate cell type-specific Cre-driver mouse lines, Surprisingly, while such a characterization has been performed for the dorsal striatum (18), it has yet to be performed for the NAc. We then examine cocaine-induced changes in dendritic spine density in input region cells, which specifically contact NAc D1- or D2-MSNS, at several distinct time points following chronic cocaine administration. Our findings suggest that cocaine-induced structural changes in neurons sending inputs to NAc are highly specific and depend both on the MSN subtype that they contact and the time point at which they are analyzed following cocaine administration.

Materials and Methods

Animals

All procedures to maintain and use mice were approved by the Institutional Animal Care and Use Committee (IACUC) at the University of California, San Diego. Mice were maintained on a 12-h:12-h light: dark cycle with regular mouse chow and water ad libitum. Adult male and female Adora2a-cre (GENSAT 036158-UCD, for labelling of D2-MSNs) and Drd1a-cre (GENSAT 017264-UCD, for labelling of D1-MSNs) congenic mice on a C57BL6/JL background were obtained from GENSAT (Gene Expression Nervous System Atlas) and backcrossed with wild type C57BL mice for several generations. Animals were randomly assigned to either control or experimental groups. Surgeries were performed between 10–12 weeks of age.

Virus generation

All AAV vectors used in this study were packaged as serotype DJ and generated as previously described (19). In brief, AAV vectors were produced by transfection of AAV293 cells (Agilent) with three plasmids: an AAV vector plasmid carrying target constructs (DIO-tdTomato-P2A-TVA, AAV-DIO-RVG), AAV helper plasmid (pHELPER; Agilent), and AAV rep-cap helper plasmid (pRC-DJ, gift from M. Kay). At 72 h post-transfection, the cells were collected and lysed by a repeated freeze-thaw procedure. Viral particles were then purified by an iodixanol step-gradient ultracentrifugation and subsequently concentrated using a 100-kDa molecular cutoff ultrafiltration device (Millipore). The genomic titer was determined by quantitative PCR. The AAV vectors were diluted in PBS to a working concentration of approximately 10^{13} viral particles/mL.

Rabies virus was designed and generated as previously described (20). In brief, B7GG cells were transfected with a total of five plasmids: four plasmids expressing the viral components pcDNA-SADB16N, pcDNA-SADB16P, pcDNA-SADB16L, pcDNA-SADB16G and a full-length cDNA plasmid containing all components of the virus where the glycoprotein coding sequence is replaced by eGFP (a gift from Karl-Klaus Conzelmann). The virus-containing media was collected 3–4 days post-transfection and used for further amplification. Viral particles were harvested from the media by centrifugation using SureSpin630 rotor at 20,000 rpm for 2 h. Rabies viral particles were reconstituted from the pellets with PBS and immediately stored at −80 °C.

To generate EnvA-pseudotyped, glycoprotein-deleted rabies virus expressing eGFP (RVΔG-eGFP(EnvA)), we used a modified version of a published protocol(20). Plasmids expressing the rabies viral components, B7GG, BHK-EnvA and HEK-TVA cells were gifts from Edward M. Callaway.

Surgeries

Mice were anesthetized with a mixture of ketamine (*75 mg/kg*) and dexmedetomidine (*0.5 mg/kg*) and placed in a stereotaxic apparatus (David Kopf Instruments). All viruses were intracranially infused at a rate of 100 nL/min using a Harvard Apparatus syringe pump into the right NAc core with coordinates relative to bregma: anterior/posterior +1.5, medial/lateral +1.0, dorsal/ventral (measured from top of skull) −4.4. The scalp was immediately resealed using a dissolvable surgical sutures (Ethicon).

For the 5 day cocaine group and saline control group, AAV-DIO-tdTomato-TVA and AAV-DIO-RVG were diluted in a 1:1:8 mixture with PBS. 250 nL of the diluted mixture was injected unilaterally into the right NAc core 14 days prior to the first cocaine injection. Two days prior to the first saline habituation injection, 250 nL RVΔG-eGFP(EnvA) was injected into the same location and the animal sacrificed 24 hours after the final cocaine or saline injection.

For reinstatement groups, 250 nL of the same diluted mixture of AAV-DIO-tdTomato-TVA and AAV-DIO-RVG was injected into the NAc core 2 days prior to the first saline habituation injection. Then, 8 days before the reinstatement shot, RVΔG-eGFP(EnvA) was injected into the same location and the animal perfused 24 hours following reinstatement

challenge. These regiments were used to ensure the same time for RVΔG-eGFP(EnvA) expression between acute and reinstatement groups.

Locomotor sensitization

All tests were conducted in a 27.25 × 27.25 cm open field arena with plain white opaque walls. Prior to acute cocaine or saline administration, all groups were given two consecutive days of a single i.p. saline injection for habituation. After 2 days of habituation, animals were given one shot of either saline or cocaine (*20 mg/kg*) once per day for five consecutive days and locomotion monitored. Animals were re-weighed each day prior to behavior in order to account for potential fluctuations in weight. After all injections, animals were immediately placed into the open field arena and locomotion was monitored using BIOBSERVE automated behavioral analysis software for 15 minutes. Animals were all injected at the same time of day ± 2 hours and sacrificed 24 hours after final injection.

For reinstatement groups, animals were injected daily *20 mg/kg* cocaine for 5 consecutive days at the same time ± 2 hours and monitored for locomotor sensitization. The animals then underwent a 2 week withdrawal in their home cage in which no saline or cocaine was administered. After 2 weeks withdrawal, a single *20 mg/kg* cocaine or saline challenge (cocaine reinstatement and saline reinstatement groups, respectively) shot was administered. Animals were again sacrificed 24 hours later. For behavior, all animals were singly housed.

Spine imaging and quantitation

Secondary dendrites were identified and imaged under an Olympus Fluoview FV1200 confocal microscope using a 100× objective (1.4 NA) at 3.5× zoom with a resolution of 1024×1024 in which each pixel corresponded to 0.035 × 0.035 × 0.15 μm. Z-stacks containing dendrites were acquired on FV10-ASW software. A high sensitive gallium arsenide phosphide (GaAsP) detector was used in most cases to ensure complete visualization of all spines. For more accurate quantitation and future morphological analysis, images were post-processed with AutoQuant X3 deconvolution software prior to analysis.

Deconvolved images were imported and analyzed through NeuronStudio (25). The software allows for automated and unbiased spine counting and spine type classification; however, to ensure accurate counting and classification, a human experimenter manually verified each spine. All imaging and quantitation was performed blind to the experimental condition and genotype.

Whole brain input quantitation

Cell counting for whole-brain input quantitation was performed as previously described (21). Briefly, mice were deeply anesthetized with isoflurane and intracardially perfused with ice cold PBS. Brains were extracted and post-fixed overnight with 4% paraformaldehyde at 4°C. After wash with PBS, the entire brain was sectioned into 60 μm coronal slices on a Leica VT1000s vibratome and immediately mounted on slides with mounting medium with DAPI. Brains were imaged at 10X on an Olympus VS120 slide scanning microscope. Every third section across the antero-posterior axis was quantified and all GFP-positive neurons were counted with the exclusion of those at the injection site (all local inputs in NAc or

starter cells were not included). Double-labeled starter cells were verified to primarily localize to NAc (Supplemental Figure S1). Animals were excluded if significant spread outside of NAc existed. Brain regions were determined by anatomical landmarks and based on Mouse Brain Atlas in Stereotaxic Coordinates, Franklin and Paxinos, 2nd edition. Quantitation is represented as total number of inputs in a brain region normalized to all inputs quantified across the entire brain (excluding NAc injection site).

Brain regions were clustered into generalized umbrella regions for Figure 1 and further refined into subregions in Figure 2, Supplemental Figure S2. Brain areas with < 1% of total inputs were not included in graphs. If not delineated in Figure 2 or Supplemental Figure S2, the following brain regions were clustered as follows (all these regions exhibited inputs to NAc):

Olfactory areas: lateral olfactory tract, olfactory tubercle, piriform cortex, rostral ventral olfactory areas.

Pallidum: ventral pallidum, interstitial nucleus of the anterior commissure, ventral diagonal band, magnocellular preoptic nucleus, horizontal diagonal band, substantia innominata, lateral globus pallidus

Hippocampus: CA1, CA3, Subiculum, amygdalohippocampal area (Ahi).

Midbrain: ventral tegmental area (VTA), periaqueductal grey (PAG), dorsal raphe nucleus (DRN), median raphe nucleus (MnR), pedunculopontine tegmental nucleus (PPTg), substantia nigra pars compacta (SNc), substantia nigra pars reticulate (SNr), interpeduncular nucleus (IP), premammillary nucleus (PMD).

Results

Viral labeling of inputs to D1-MSNs and D2-MSNs in NAc

To identify all brain-wide cells sending monosynaptic inputs specifically to either NAc D1- or D2-MSNs in an unbiased fashion, we used a viral tracing strategy that depends on a glycoprotein-deleted EnvA-pseudotyped rabies virus (Figure 1A; (22)). First, we expressed an exogenous avian receptor for the EnvA ligand (TVA) in either D1- or D2-MSNs by injecting adeno-associated virus (AAV) expressing TVA receptor together with the red fluorescent protein, tdTomato, (AAV-DIO-tdTomato-TVA) in a Cre-recombinase dependent manner into the NAc core of D1-Cre or A2A-Cre mice (for labelling of D1- or D2-MSNs, respectively). We simultaneously supplied the rabies virus glycoprotein (RVG) *in trans* by also injecting AAV-DIO-RVG into the NAc core as well. After waiting 14 days to allow adequate TVA receptor and RVG expression, we injected glycoprotein-deleted EnvA-pseudotyped rabies conjugated to eGFP (EnvA-RVΔG-eGFP) and after waiting an additional 7 days, processed the brains for unbiased brain-wide analysis of labeled neurons (Figure 1B; (22, 23)). Using this method, the tdTomato- and GFP-positive neurons in the NAc are known as “starter neurons”, which are the postsynaptic partners of monosynaptically connected input neurons that are retrogradely labeled with only GFP (Figure 1C; Supplemental Figure S1).

Brain-wide quantitation of all inputs to NAc D1- or D2-MSNs revealed quantitatively similar proportions of labelled input neurons to both MSN cell types from general brain areas such as cortex and hippocampus, although D2-MSNs received proportionally, but not significantly, stronger inputs from the amygdala and pallidum (Figure 1C, D). Strikingly, we find that the NAc MSNs receive direct synaptic input from over 50 distinct subregions across the brain. Closer examination of subregions within the cortex revealed that D1-MSNs receive significantly more input from medial orbitofrontal cortex (MO), yet similar proportions of inputs from prelimbic (PrL) and infralimbic (IL) cortex (Figure 2A, B), which are components of the mPFC that have been implicated in playing important roles in cocaine use (24, 25). Interestingly, we found that across all individual brain regions, D2-MSNs received the greatest input from the PVT (Figure 2C, D), suggesting that this pathway may be more critical to the function of NAc D2-MSNs than previously thought (26) (Figure 2C).

Since our tracing results revealed a strong trend of D2-MSNs receiving more input from the amygdaloid complex, we reasoned that different subdivisions of the amygdala may have a difference in their projection preference. However, closer examination revealed no statistical difference in the inputs from lateral or central amygdalar subnuclei to either NAc D1- or D2-MSNs (Figure 2E, F). Additionally, no quantitative differences in the proportion of inputs onto D1- and D2-MSNs were observed in hypothalamic, pallidal, or hippocampal subregions (Supplemental Figure S2A-C, data not shown). Collectively, we find that D1- and D2-MSNs receive overall quantitatively similar brain-wide inputs, with the lone exception that D1-MSNs receive significantly more input from MO cortex.

Input labeling at different stages of cocaine administration

Spines are small structural protrusions of dendrites known to be sites of excitatory synaptic contact due to the high concentrations of PSD-95 protein, AMPA receptors, and NMDA receptors. Disruption of their formation has been shown to lead to profound synaptic and functional deficits (27, 28). Changes in spine density and composition may thus serve as a useful structural proxy for synaptic alterations at the cellular level. Previous reports indicate that dendritic spines of NAc D1- and D2-MSNs exhibit differential plasticity after chronic cocaine administration (29–31). It is unknown, however, whether this spine plasticity extends to neurons sending projections to the NAc and if this plasticity changes during the course of cocaine administration and withdrawal from cocaine. To address this topic, we used the viral strategy described above and also asked whether cocaine-induced spine plasticity in input neurons differed depending on whether they contacted D1- or D2-MSNs.

After NAc injection of the TVA and RVG expressing AAV's, mice received one of four treatments: 1) one injection of saline per day for five days (5d saline), 2) one injection of cocaine per day (20 mg/kg) for five days (5d cocaine), 3) daily injection of cocaine (20 mg/kg) for five days followed by a 2 week withdrawal period with a single injection of saline on withdrawal day 14 (saline reinstatement), 4) same as 3, except a single shot of cocaine (20 mg/kg) was given on withdrawal day 14 (cocaine reinstatement; Figure 3A, B). For treatments 1 and 2, NAc rabies virus injections were made the day before the 5 day treatment regime; for treatments 3 and 4, rabies virus was injected into the NAc on withdrawal day 7 (Figure 3A, B). These regimens were chosen because they are similar to

those used previously to model some of the separate stages of drug abuse, discriminating the neural adaptations that occur during the initial stages of cocaine administration (acute cocaine) from those that occur during withdrawal (32, 33).

After each cocaine or saline administration, animals' locomotor activity was assayed to test cocaine's efficacy and confirm the occurrence of behavioral sensitization (34). As expected, locomotor activity increased over successive cocaine, but not successive saline, injections (Figure 3C, D). Locomotor activity in the cocaine reinstatement group remained elevated to levels comparable to the fifth day of acute cocaine administration, suggesting that despite two weeks of withdrawal, animals retained the neural adaptations that mediated the enhanced locomotor response to cocaine.

BLA neurons projecting to NAc MSNs are differentially affected by cocaine

Since differential changes in synaptic strength at the BLA, vHPC, and mPFC inputs to NAc D1- and D2-MSNs in response to cocaine administration have been previously described, we focused our spine analysis on these input regions (10, 29). Additionally, since our tracing analysis identified the MO as one of the brain regions preferentially targeting D1-MSNs over D2-MSNs, we included this area in our analysis as well. Input neurons were easily identified by the presence of GFP, which allowed collection of high-resolution confocal z-stack images of secondary dendritic branches and high-precision quantitation of spine density and spine morphological subtype at different stages of cocaine administration. Unbiased 3D spine morphometric analysis was performed using NeuronStudio software semi-automatically and manually double-checked and adjusted in a blinded fashion (35).

We observed that BLA neurons projecting to NAc D1-MSNs, but not D2-MSNs exhibited distinct changes in dendritic spine density in all treatment groups that received cocaine (Figure 3E-G). Specifically, spine density of BLA neurons projecting to NAc D1-MSNs increased after 5 days of cocaine injections and continued to increase after 14 days of withdrawal with both saline and cocaine reinstatement injections (Figure 3E-G). In marked contrast, BLA neurons projecting to NAc D2-MSNs exhibited no significant changes in spine density due to cocaine administration (Figure 3I, J). These results parallel a previous report suggesting that BLA synapses on NAc D1-, but not D2-MSNs exhibit an increase in synaptic strength after 5 days of cocaine administration (10).

Spines can be further classified based on their individual morphology as thin, stubby, or mushroom-shaped, each thought to represent differing levels of maturation and plasticity (27, 36). Thus, we next analyzed whether specific spine subtypes in BLA neurons displayed dynamic plasticity in response to cocaine administration based on their target neurons in NAc. Five days of cocaine treatment followed by a withdrawal period resulted in a significant decrement in the relative number of thin spines and a concomitant increase in the number of mushroom spines in D1-MSN projecting BLA neurons (Supplemental Figure S3A). This may reflect maturation of thin spines to mushroom spines during the withdrawal period (37). Although no net change in overall spine density was observed in BLA neurons projecting to D2-MSNs, a dynamic rearrangement of the relative proportion of the three spines subtypes was observed (Supplemental Figure S3B). This rearrangement of different spine subtypes may offset each other, thereby resulting in the observed lack of net change in

average spine density. Together, these results demonstrate distinct types of cocaine-induced structural plasticity in NAc-projecting BLA neurons based on their target cell types in NAc.

Dendritic spine density increases in D1-MSN projecting vHPC neurons after 14 day withdrawal

Ventral hippocampal (vHPC) neurons projecting to NAc, mostly located in the subiculum subregion, have prominent apical and basal dendritic structures (38). It has been suggested that discrete regions of dendrites receive inputs from different brain structures and can exhibit differential plasticity (39, 40). To account for this, we analyzed spine density in both subregions of these neurons' dendritic tree – apical and basal dendrites. Unlike NAc-projecting BLA neurons, 5 day acute cocaine administration caused no detectable changes in spine density on apical or basal dendrites of vHPC neurons projecting to either D1-MSNs or D2-MSNs (Figure 4). However, after cocaine administration following two weeks of withdrawal we observed an increase in spine density in both apical and basal dendrites of vHPC neurons projecting to D1-MSNs, but not to D2-MSNs (Figure 4). We observed a trend towards a reduction in the relative proportion of stubby spines in vHPC apical dendrites projecting to D1-, but not D2-MSNs, after 2 week withdrawal from cocaine; however, this did not reach significance (Supplemental Figure 3C, D). Similarly, basal dendrites in vHPC neurons projecting to D1-MSNs exhibited a significant decrease in the proportion of stubby spines after the 14 day withdrawal period in both reinstatement groups suggesting that this dynamic spine subtype remodeling may not depend on the NAc cell-type it targets (Supplemental Figure S3E, F). Thus, similar to NAc-projecting BLA neurons, dendrites on vHPC neurons display differential structural plasticity dependent on the target NAc cell-type.

Cocaine administration induces a decrease in spine density of PrL neurons projecting to D1-MSNs, but not D2-MSNs

Like vHPC neurons, PrL neurons projecting to NAc also have long, elaborated dendritic structures along the different layers of prelimbic cortex (41). Since different layers of the cortex receive inputs from different brain areas, we again separately examined apical dendritic spines, which are located in the lower, more superficial layers of cortex, and basal dendrites located in the higher, deeper layers of cortex. In contrast to NAc-projecting BLA and vHPC neurons, cocaine administration followed by two weeks of withdrawal induced a decrease in spine density in apical dendrites of PrL neurons innervating D1-MSNs (Figure 5A-C). Although we observed a trend, 5 days of cocaine administration was not sufficient to induce a reduction in apical spine density in this group. Despite observing a decrease in average spine density, these changes were not accompanied by significant changes in spine subtypes (Supplemental Figure S4A).

While we observed changes in apical dendrite spine density of PrL neurons projecting to D1-MSNs in response to cocaine administration, no change was observed in D2-MSN projecting PrL neuronal apical dendrites (Figure 5D, E). Interestingly, despite no net changes in density, we observed dynamic structural reorganization of individual spines on apical dendrites evidenced by alterations in thin and stubby spine ratios: apical dendrites

exhibited a decrease in thin spines after 5 days cocaine administration and a proportional increase in stubby spines (Supplemental Figure S4B).

Basal dendrites on D1-MSN projecting PrL neurons displayed a more pronounced effect, as the average spine density decreased after 5 days cocaine exposure and persisted after 14 days of withdrawal with both saline and cocaine reinstatement shots (Figure 5F-H). However, consistent with the apical dendrite group, this was not accompanied by any changes in spine subtype composition (Supplemental Figure S4C). On the other hand, basal dendrites on D2-MSN projecting PrL neurons exhibited no significant changes in spine density but, similar to apical dendrites, showed dynamic spine subtype remodeling (Figure 5I, J; Supplemental Figure 4D). A decrement in thin spines was observed along with an increase in stubby spines after 5 days cocaine injection that persisted after withdrawal and a saline reinstatement shot (Supplemental Figure 4D). This increase in stubby spines may serve to offset the reduction in thin spines and could explain why we observed no significant difference in average spine density.

Cocaine administration decreases spine density in dendrites of MO inputs to both D1-MSNs and D2-MSNs

The MO and the PrL, collectively known as the medial prefrontal cortex, are known to exhibit different anatomical connections and functions (42–44). Additionally, our anatomical analysis revealed that D1-MSNs received proportionally more input from NAc-projecting MO neurons compared to D2-MSNs (Figure 2A). For these reasons, we decided to subdivide these regions in our analysis to see if cocaine administration may differentially affect them. Spine quantitation revealed a significant reduction in density of both basal and apical dendrites in MO neurons projecting to D1-MSNs after 5 days of cocaine administration, similar to what was observed in the PrL cortex (Figure. 6A-C, F-G). However, unlike PrL neurons projecting to D2-MSNs which showed no change, we observed a significant reduction in spine density of MO neurons projecting to D2-MSNs in both apical and basal dendrites after 5 days of cocaine administration as well (Figure 6D, E, I, H). Interestingly, while the MO was an area we identified as sending more proportional inputs to D1-MSNs, this was the only brain region projecting to D2-MSNs in which we measured significant changes in spine density (Figure 6I, H). This reduction is driven primarily through reduced mushroom-type spines (Supplemental Figure S4E-H). The decrease in spine density after acute cocaine administration was not sustained after 14 days of withdrawal, as both saline and cocaine reinstatement groups had spine density levels similar to saline controls. Collectively, these data indicate that MO neurons projecting to NAc show a non-discriminatory decrease in spine density after 5 days cocaine administration.

Discussion

Brain-wide anatomical organization of NAc D1- and D2-MSN specific inputs

Here, using virus-mediated circuit mapping together with transgenic mice expressing Cre-recombinase in specific cell types, we characterize the brain-wide distributions of afferent inputs to D1-MSNs and D2-MSNs in the NAc core. While previous studies have provided a

basic framework of synaptic organizations of D1- and D2-MSNs and their different roles, no study has provided a thorough delineation of brain-wide inputs to specific cell types in NAc (10, 13, 29). We find that over 50 distinct brain subregions provide direct synaptic inputs onto NAc MSNs, a finding that presumably reflects the critical importance of the NAc in integrating very diverse types of information in the service of its role in translating motivation into action (45).

Surprisingly, in contrast to the distinct functional roles ascribed to D1-MSNs and D2-MSNs, our trans-synaptic tracing demonstrate largely non-discriminatory monosynaptic innervation to the two-different populations in NAc core across the antero-posterior axis of the brain (Figure 1). One exception is that D1-MSNs receive significantly more inputs than D2-MSNs from NAc-projecting MO neurons (Figure 2A, B). We also find a strong trend of increased input to D2-MSNs over D1-MSNs from the amygdala and paraventricular nucleus of the thalamus (Figure 2C, D). This strong, but non-significant trend, may reflect the fact that a substantial fraction of D1-MSNs show the same output projection pattern as that of D2-MSNs, sending projections to the ventral pallidum (VP) rather than to the VTA (46). These populations of VP-projecting D1-MSNs and D2-MSNs may share similar brain-wide inputs, in contrast to VTA-projecting D1-MSNs. Further analysis using additional methods will be required to differentiate inputs to distinct populations of D1-MSNs projecting to VTA or VP (47).

Previous reports have identified separate input patterns, functions, and structural changes based on whether MSNs are located in the NAc core, medial shell, or lateral shell (30, 48). Since our circuit analysis is limited to inputs to the NAc core, it remains plausible that significant differences in afferent organization between D1- and D2-MSNs exist in the NAc medial or lateral shell. Future work will be required to dissect the input patterns to D1- and D2-MSNs in separate sub-compartments of the NAc.

Although the mPFC, vHPC, and BLA are the most heavily studied inputs to the nucleus accumbens, our brain-wide analysis revealed that the paraventricular nucleus of the thalamus (PVT) sends proportionally more input to the NAc than any other brain area, especially to D2-MSNs. While recent studies have begun to focus on the PVT-NAc circuit (26, 49), future studies are required to further uncover its functional roles, particularly as it pertains to differential plasticity compared to mPFC, vHPC, and BLA afferents to the NAc. Indeed, recent studies have reported separate changes in synaptic plasticity in the PVT-NAc circuit after cocaine withdrawal compared to BLA- and mPFC-NAc circuits (26, 50). Furthermore, the large number of brain areas sending inputs to NAc MSNs points to the potential importance of delineating the roles of adaptations in these synapses in mediating the different stages of addiction.

Cocaine administration-induced stage-specific structural plasticity in afferent inputs to NAc

The progression to recurrent drug use initiates as recreational use, which eventually evolves into compulsive use, suggesting that distinct brain areas are engaged at different stages of drug addiction. Although it has been proposed that adaptations in upstream excitatory neurons projecting to NAc may contribute to the long-lasting drug-induced neural

adaptations in NAc (51), how those inputs are engaged at different stages of cocaine administration has not been fully addressed. We find that both repeated exposure to cocaine and exposure followed by a withdrawal period elicits robust but distinct changes in structural plasticity in neurons upstream of NAc MSNs. These changes are dependent on three key factors: 1) the brain structure which monosynaptically projects to the NAc, 2) the cell-type within the NAc that is targeted and, 3) the stage of cocaine exposure at which the spine analysis is performed..

In our first analysis we find a selective increase in spine density in BLA neurons projecting to D1-MSNs, but not D2-MSNs (Figure 3). This observation is consistent with recent work showing a selective increase in BLA innervation of D1-MSNs by repeated cocaine administration (10). Even after 14 days of abstinence structural changes persisted in D1-MSN-projecting BLA neurons suggesting that spine changes represent a lasting adaptation to repeated cocaine use and not just an acute, transient process. Future examination of how manipulation of spine dynamics may affect cocaine seeking are required. Furthermore, since BLA neurons have been shown to encode both rewarding and aversive signals (52, 53), it is possible that distinct BLA neuronal subpopulations differentially project to D1-MSNs and D2-MSNs. Further study is needed to examine the molecular and functional identity of BLA neurons that target distinct neuronal populations in NAc.

Second, the spine density of vHPC neurons projecting to D1-MSNs, but not to D2-MSNs, showed a significant increase only when animals were challenged by cocaine after 14 days withdrawal. Previous reports show that silencing vHPC neurons projecting to the NAc inhibits cocaine induced locomotor sensitization (51). Thus, the increase in spine density of vHPC neurons projecting to D1-MSNs may lie upstream of synaptic changes at the NAc MSN synapse during periods of cocaine seeking or reinstatement. This idea is also supported by studies showing that vHPC inputs to NAc are potentiated by withdrawal after repeated exposure to cocaine (51).

Third, prefrontal cortical neurons in both MO and PrL showed a significant reduction in their spine density following 5 days of cocaine administration. These findings are consistent with recent results using high resolution two-photon imaging of cortical neurons in chronic cocaine administration (54). However, this report as well as our data are not consistent with previous findings with Golgi-staining preparation (55–57). This discrepancy may be due to the nature of Golgi staining which randomly and sparsely labels neurons without a clear known mechanism together with low-magnification imaging. In contrast, our methods examine specific cortical populations projecting to distinct cell types within the NAc.

The overall increase in spine density in BLA and vHPC neurons and decrease in prefrontal (PrL and MO) spine density in response to cocaine administration may parallel the previously defined roles for these projections to the NAc. For example, since the BLA appears to encode emotional valence, it is possible that the acute increase in spine density is necessary to form the initial affective response to cocaine, which often persists after withdrawal. On the other hand, vHPC spine density only increased 14 days after withdrawal and after a cocaine challenge. Since the vHPC is thought to link experience with contextual information (58) it is plausible that the 14 day withdrawal period is required for

strengthening the vHPC-NAc pathway to maintain the contextual representation of cocaine seeking induced during the initial 5 day cocaine administration. Finally, the decrease in spine density in the mPFC immediately following the 5 day cocaine administration period may reflect that in the developing stages of addiction, individuals experience a loss of top-down control and aberrant action-outcome evaluation, both of which are associated with mPFC activity (42).

An important general conclusion is that, in general, spines on D1-MSN projecting neurons appear to be more plastic than D2-MSN projecting neurons in all the brain structures that we examined. This likely reflects the different roles that these two major cell types play in mediating the behavioral functions of the NAc. Our results also highlight the pressing need for increased specificity in regards to cell-type, brain-area, and stage-specific aspects of neural adaptations in response to drugs of abuse such as cocaine. While the majority of studies have focused on structural and synaptic adaptations within NAc MSNs, our results demonstrate that potentially important structural changes occur in upstream brain regions. Clearly, further study of the many different upstream neuronal populations that influence NAc activity is needed for a more comprehensive understanding of the neural adaptations underlying complex neuropsychiatric disorders such as addiction.

Supplementary Material

Refer to Web version on PubMed Central for supplementary material.

Acknowledgements

We thank X. Wang for technical assistance, H. Pribiag and Lim laboratory for comments on manuscript. This work was supported by Klingenstein foundation, Searle scholar program (Kinship foundation), Whitehall foundation, and grants from NIH (DA040030, DA008227). V.L. is also supported by Anandamahidol Foundation Fellowship.

References

1. Lüscher C, Malenka RC (2011): Drug-Evoked Synaptic Plasticity in Addiction: From Molecular Changes to Circuit Remodeling. Neuron. 69: 650–663. [PubMed: 21338877]
2. Grueter B a, Rothwell PE, Malenka RC (2012): Integrating synaptic plasticity and striatal circuit function in addiction. Curr Opin Neurobiol. 22: 545–51. [PubMed: 22000687]
3. Kalivas PW, Volkow ND (2005): The Neural Basis of Addiction:A Pathology of Motivation and Choice. Am J Psychiatry. 162: 1403–1413. [PubMed: 16055761]
4. Nestler EJ (2001): Molecular Basis of Long-term Plasticity Underlying Addiction. Nat Rev Neurosci. 2: 119–128. [PubMed: 11252991]
5. Russo SJ, Dietz DM, Dumitriu D, Morrison JH, Malenka RC, Nestler EJ (2010): The addicted synapse: mechanisms of synaptic and structural plasticity in nucleus accumbens. Trends Neurosci. 33: 267–76. [PubMed: 20207024]
6. Olds J, Milner P (1954): Positive reinforcement produced by electrical stimulation of septal area and other regions of rat brain.
7. Al-Hasani R, McCall JG, Shin G, Gomez AM, Schmitz GP, Bernardi JM, et al. (2015): Distinct Subpopulations of Nucleus Accumbens Dynorphin Neurons Drive Aversion and Reward. Neuron. 87: 1063–1077. [PubMed: 26335648]
8. Le Moine C, Bloch B (1995): D1 and D2 dopamine receptor gene expression in the rat striatum: Sensitive cRNA probes demonstrate prominent segregation of D1 and D2 mRNAS in distinct neuronal populations of the dorsal and ventral striatum. J Comp Neurol. 355: 418–426. [PubMed: 7636023]

9. Lobo MK, Covington HE, Chaudhury D, Friedman AK, Sun H, Damez-Werno D, et al. (2010): Cell Type-Specific Loss of BDNF Signaling Mimics Optogenetic Control of Cocaine Reward. Science (80-). 327: 385–391.
10. MacAskill AF, Cassel JM, Carter AG (2014): Cocaine exposure reorganizes cell type– and input-specific connectivity in the nucleus accumbens. Nat Neurosci. 17: 1198–1207. [PubMed: 25108911]
11. Lee K-W, Kim Y, Kim AM, Helmin K, Nairn AC, Greengard P (2006): Cocaine-induced dendritic spine formation in D1 and D2 dopamine receptor-containing medium spiny neurons in nucleus accumbens. Proc Natl Acad Sci U S A. 103: 3399–404. [PubMed: 16492766]
12. Bock R, Shin JH, Kaplan AR, Dobi A, Markey E, Kramer PF, et al. (2013): Strengthening the accumbal indirect pathway promotes resilience to compulsive cocaine use. Nat Neurosci. 16: 632–8. [PubMed: 23542690]
13. Creed M, Ntamati NR, Chandra R, Lobo MK, Lüscher C (2016): Convergence of Reinforcing and Anhedonic Cocaine Effects in the Ventral Pallidum. Neuron. 214–226.
14. Nestler EJ (2004): Historical review: Molecular and cellular mechanisms of opiate and cocaine addiction. Trends Pharmacol Sci. 25: 210–218. [PubMed: 15063085]
15. Russo SJ, Nestler EJ (2013): The brain reward circuitry in mood disorders. Nat Rev Neurosci. 14: 609–25. [PubMed: 23942470]
16. Zhu Y, Wienecke CFR, Nachtrab G, Chen X (2016): A thalamic input to the nucleus accumbens mediates opiate dependence. Nature. 530. doi: 10.1038/nature16954.
17. Kalivas PW, O'Brien C (2008): Drug addiction as a pathology of staged neuroplasticity. Neuropsychopharmacology. 33: 166–80. [PubMed: 17805308]
18. Wall N, DeLaParra M, Callaway E, Kreitzer A (2013): Differential innervation of direct- and indirect-pathway striatal projection neurons. Neuron. 79: 347–360. [PubMed: 23810541]
19. Lim BK, Huang KW, Grueter B a, Rothwell PE, Malenka RC(2012): Anhedonia requires MC4R-mediated synaptic adaptations in nucleus accumbens. Nature. 487: 183–9. [PubMed: 22785313]
20. Osakada F, Callaway EM (2013): Design and generation of recombinant rabies virus vectors. Nat Protoc. 8: 1583–601. [PubMed: 23887178]
21. Knowland D, Lilascharoen V, Pham Pacia C, Shin S, Hou-Jen Wang E, Kook Lim B (2017): Distinct Ventral Pallidal Neural Populations Mediate Separate Symptoms of Depression. Cell. 170: 1–14. [PubMed: 28666111]
22. Wickersham IR, Lyon DC, Barnard RJO, Mori T, Finke S, Conzelmann K-K, et al. (2007): Monosynaptic restriction of transsynaptic tracing from single, genetically targeted neurons. Neuron. 53: 639–47. [PubMed: 17329205]
23. Wall NR, Wickersham IR, Cetin A, De La Parra M, Callaway EM (2010): Monosynaptic circuit tracing in vivo through Cre-dependent targeting and complementation of modified rabies virus. Proc Natl Acad Sci U S A. 107: 21848–53. [PubMed: 21115815]
24. Miller CA, Marshall JF (2004): Altered Prelimbic Cortex Output during Cue-Elicited Drug Seeking. J Neurosci. 24: 6889–6897. [PubMed: 15295023]
25. Winstanley CA, Bachtell RK, Theobald DEH, Laali S, Green TA, Kumar A, et al. (2009): Increased impulsivity during withdrawal from cocaine self-administration: Role for ??FosB in the orbitofrontal cortex. Cereb Cortex. 19: 435–444. [PubMed: 18539927]
26. Neumann PA, Wang Y, Yan Y, Wang Y, Ishikawa M, Cui R, et al. (2016): Cocaine-Induced Synaptic Alterations in Thalamus to Nucleus Accumbens Projection. Neuropsychopharmacology. 41: 2399–2410. [PubMed: 27074816]
27. Hering H, Sheng M (2001): Dentritic spines: structure, dynamics and regulation. Nat Rev Neurosci. 2: 880–888. [PubMed: 11733795]
28. Vogl AM, Brockmann MM, Giusti SA, MacCarrone G, Vercelli CA, Bauder CA, et al. (2015): Neddylation inhibition impairs spine development, destabilizes synapses and deteriorates cognition. Nat Neurosci. 18: 239–251. [PubMed: 25581363]
29. MacAskill AF, Little JP, Cassel JM, Carter AG (2012): Subcellular connectivity underlies pathway-specific signaling in the nucleus accumbens. Nat Neurosci. 15: 1624–6. [PubMed: 23143514]

30. Dumitriu D, Laplant Q, Grossman YS, Dias C, Janssen WG, Russo SJ, et al. (2012): Subregional, dendritic compartment, and spine subtype specificity in cocaine regulation of dendritic spines in the nucleus accumbens. J Neurosci. 32: 6957–66. [PubMed: 22593064]

31. Dobi A, Seabold GK, Christensen CH, Bock R, Alvarez V a (2011): Cocaine-induced plasticity in the nucleus accumbens is cell specific and develops without prolonged withdrawal. J Neurosci. 31: 1895–904. [PubMed: 21289199]

32. Kourrich S, Rothwell PE, Klug JR, Thomas MJ (2007): Cocaine Experience Controls Bidirectional Synaptic Plasticity in the Nucleus Accumbens. J Neurosci. 27: 7921–7928. [PubMed: 17652583]

33. Rothwell PE, Kourrich S, Thomas MJ (2011): Synaptic adaptations in the nucleus accumbens caused by experiences linked to relapse. Biol Psychiatry. 69: 1124–6. [PubMed: 21329910]

34. Sanchis-segura C, Spanagel R (2006): Behavioural assessment of drug reinforcement and addictive features in rodents : an overview. Addict Biol. 2–38. [PubMed: 16759333]

35. Rodriguez A, Ehlenberger DB, Dickstein DL, Hof PR, Wearne SL (2008): Automated three-dimensional detection and shape classification of dendritic spines from fluorescence microscopy images. PLoS One. 3. doi: 10.1371/journal.pone.0001997.

36. Peters A, Kaiserman-Abramof IR (1970): The small pyramidal neuron of the rat cerebral cortex. The perikaryon, dendrites and spines. Am J Anat. 127: 321–355. [PubMed: 4985058]

37. Nimchinsky EA, Sabatini BL, Svoboda K (2002): Structure and function of dendritic spines. Annu Rev Physiol. 64: 313–353. [PubMed: 11826272]

38. Harris E, Witter MP, Weinstein G, Stewart M (2001): Intrinsic connectivity of the rat subiculum: I. Dendritic morphology and patterns of axonal arborization by pyramidal neurons. J Comp Neurol. 435: 490–505. [PubMed: 11406828]

39. Makara JK, Losonczy A, Wen Q, Magee JC (2009): Experience-dependent compartmentalized dendritic plasticity in rat hippocampal CA1 pyramidal neurons. Nat Neurosci. 12: 1485–1487. [PubMed: 19898470]

40. Losonczy A, Makara JK, Magee JC (2008): Compartmentalized dendritic plasticity and input feature storage in neurons. Nature. 452: 436–441. [PubMed: 18368112]

41. Radley JJ, Rocher AB, Rodrigues A, Ehlenberger DB, Dammann M, Mcewen BS, et al. (2008): Repeated Stress Alters Dendritic Spine Morphology in the Rat Medial Prefrontal Cortex. J Comp Neurol. 507: 1141–1150. [PubMed: 18157834]

42. Volkow ND, Fowler JS (2000): Addiction, a disease of compulsion and drive: involvement of the orbitofrontal cortex. Cereb Cortex. 10: 318–25. [PubMed: 10731226]

43. Capriles N, Rodaros D, Sorge RE, Stewart J (2003): A role for the prefrontal cortex in stress- and cocaine-induced reinstatement of cocaine seeking in rats. Psychopharmacology (Berl). 168: 66–74. [PubMed: 12442201]

44. Boulougouris V, Dalley JW, Robbins TW (2007): Effects of orbitofrontal, infralimbic and prelimbic cortical lesions on serial spatial reversal learning in the rat. Behav Brain Res. 179: 219–228. [PubMed: 17337305]

45. Mogenson GJ, Jones DL, Yim CY (1980): From motivation to action: Functional interface between the limbic system and the motor system. Prog Neurobiol. 14: 69–97. [PubMed: 6999537]

46. Kupchik YM, Brown RM, Heinsbroek J a, Lobo MK, Schwartz DJ, Kalivas PW(2015): Coding the direct/indirect pathways by D1 and D2 receptors is not valid for accumbens projections. Nat Neurosci. 18: 1230–1232. [PubMed: 26214370]

47. Schwarz L a., Miyamichi K, Gao XJ, Beier KT, Weissbourd B, DeLoach KE, et al. (2015): Viral-genetic tracing of the input–output organization of a central noradrenaline circuit. Nature. doi: 10.1038/nature14600.

48. Lammel S, Hetzel A, Häckel O, Jones I, Liss B, Roeper J (2008): Unique Properties of Mesoprefrontal Neurons within a Dual Mesocorticolimbic Dopamine System. Neuron. 57: 760–773. [PubMed: 18341995]

49. Wunsch AM, Yager LM, Donckels EA, Le CT, Neumaier JF, Ferguson SM (2017): Chemogenetic inhibition reveals midline thalamic nuclei and thalamo- accumbens projections mediate cocaine-seeking in rats. Eur J Neurosci. 46: 1850–1862. [PubMed: 28664636]

50. Joffe ME, Grueter BA (2016): Cocaine Experience Enhances Thalamo-Accumbens N-Methyl-D-Aspartate Receptor Function. Biol Psychiatry. 80: 671–681. [PubMed: 27209241]

51. Britt JP, Benaliouad F, McDevitt RA, Stuber GD, Wise RA, Bonci A (2012): Synaptic and Behavioral Profile of Multiple Glutamatergic Inputs to the Nucleus Accumbens. Neuron. 76: 790–803. [PubMed: 23177963]

52. Behaviors A, Kim J, Zhang X, Muralidhar S, Leblanc SA, Kim J, et al. (2017): Basolateral to Central Amygdala Neural Circuits for Appetitive Behaviors: Neuron. Neuron. 93: 1464–1479.e5. [PubMed: 28334609]

53. Beyeler A, Namburi P, Glober GF, Luck R, Wildes CP, Tye Correspondence KM, et al. (2016): Divergent Routing of Positive and Negative Information from the Amygdala during Memory Retrieval. Neuron. 90: 348–361. [PubMed: 27041499]

54. Muñoz-Cuevas FJ, Athilingam J, Piscopo D, Wilbrecht L (2013): Cocaine-induced structural plasticity in frontal cortex correlates with conditioned place preference. Nat Neurosci. 16: 1367–9. [PubMed: 23974707]

55. Robinson TE, Gorny G, Mitton E, Kolb B (2001): Cocaine Self-Administration Alters the Morphology of Dendrites and Dendritic Spines in the Nucleus Accumbens and Neocortex. Synapse. 266: 257–266.

56. Robinson TE (1999): Alterations in the morphology of dendrites and dendritic spines in the nucleus accumbens and prefrontal cortex following repeated treatment with amphetamine or cocaine. Eur J Neurosci. 11: 1598–1604. [PubMed: 10215912]

57. Li Y, Acerbo MJ, Robinson TE (2004): The induction of behavioural sensitization is associated with cocaine-induced structural plasticity in the core (but not shell) of the nucleus accumbens. Eur J Neurosci. 20: 1647–1654. [PubMed: 15355332]

58. Rogers JL, See RE (2007): Selective inactivation of the ventral hippocampus attenuates cue-induced and cocaine-primed reinstatement of drug-seeking in rats. Neurobiol Learn Mem. 87: 688–692. [PubMed: 17337218]

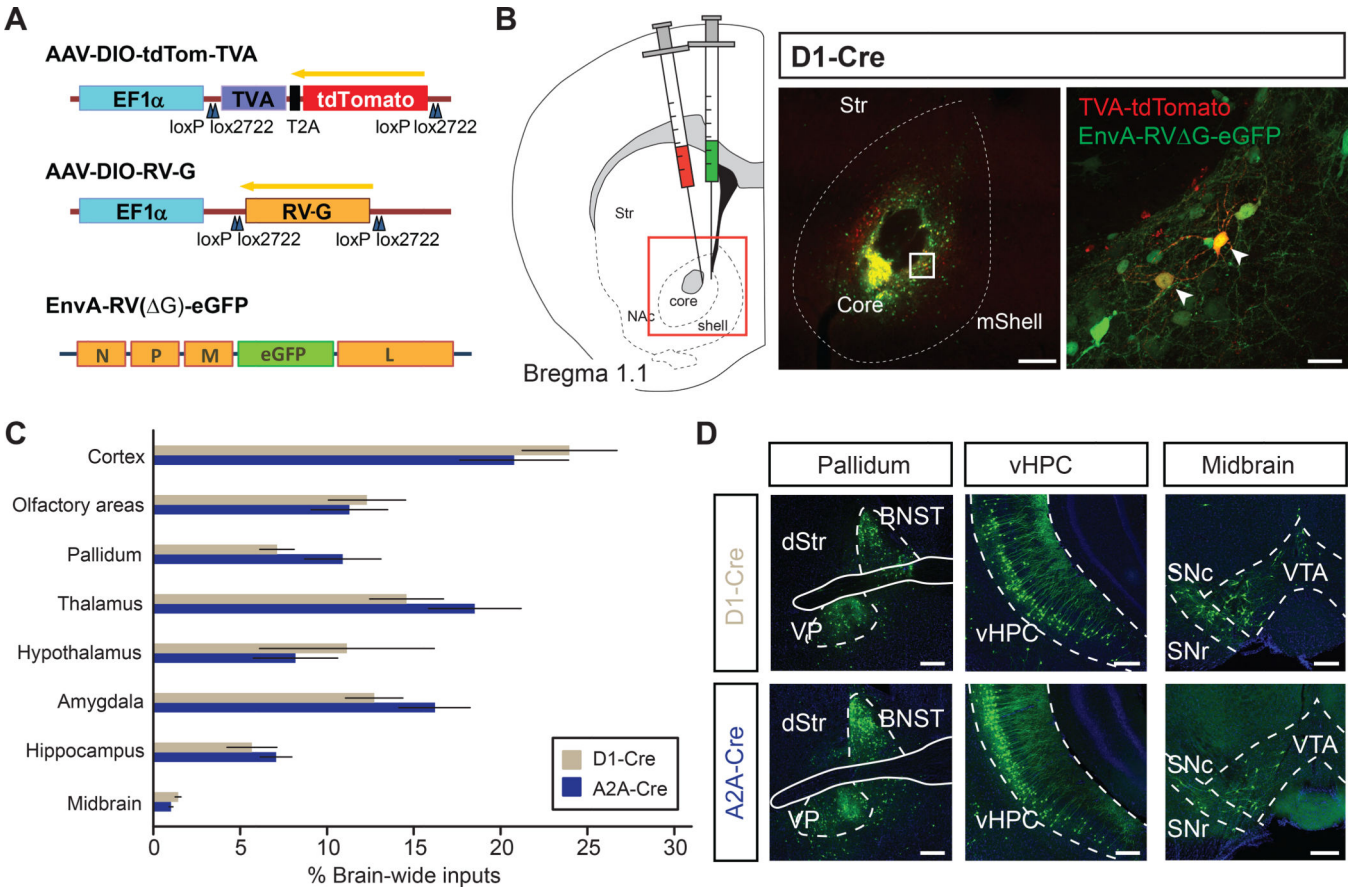

Figure 1.

Brain-wide monosynaptic inputs to NAc D1- and D2-receptor expressing medium spiny neurons (D1-MSNs, D2-MSNs, respectively)

(*A*) (*Left*) Viral vectors used to express Cre-dependent TVA receptor, rabies glycoprotein, and G-deleted EnvA-pseudotyped rabies virus (AAV-DIO-tdTom-TVA, AAV-DIO-RV-G, EnvA-RV(ΔG)-eGFP, respectively). (*Right*) Schematic of viral injections targeting NAc core.

(*B*) Injection schematic. D1-Cre or A2A-Cre mice were unilaterally injected with viruses in (*A*) into nucleus accumbens (NAc) core (left). Representative images of injection site showing colocalized 'starter cells' (right). Box denotes area of zoom. Scale bar, 200 μm (left), 25 μm (right)

(*C*) Brain-wide quantitation of inputs to D1- and D2-MSNs (D1-Cre and A2A-Cre, respectively; n = 7 for each genotype). See methods for how brain regions were clustered.

(*D*) Representative images for different input brain regions. Green cells represent individual neurons sending monosynaptic input to D1- (top row) or D2-MSNs (bottom row) in the NAc. Scale: 250 um

Abbreviations: BNST, bed nucleus stria terminalis; VP, ventral pallidum; dStr, dorsal striatum; SNc, substantia nigra pars compacta; SNr, substantia nigra pars reticulate; VTA, ventral tegmental area.

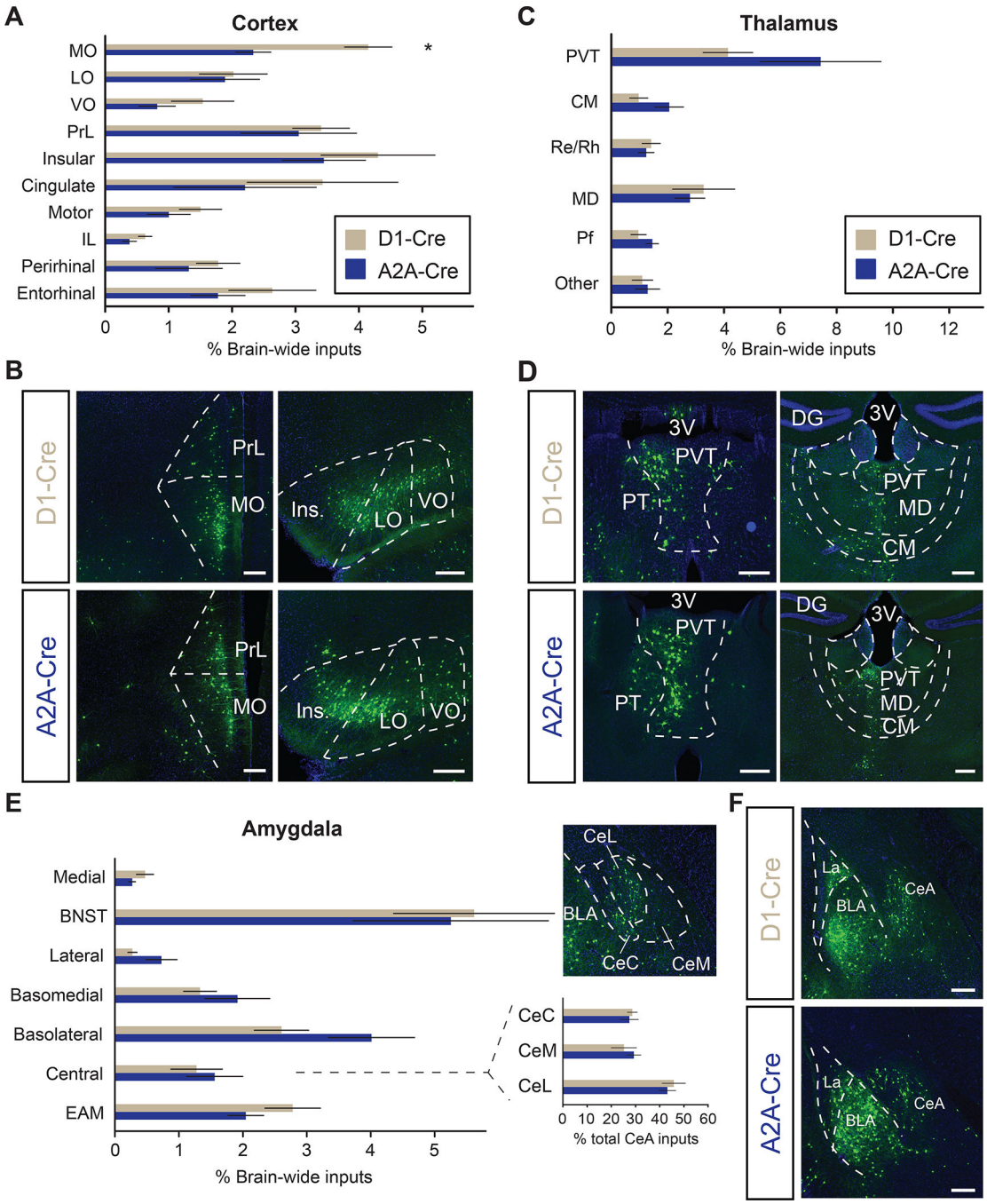

Figure 2.

D1- and D2-receptor expressing medium spiny neurons (D1-MSNs, D2-MSNs, respectively) exhibit different cortical input patterns

(*A*) Quantitation of inputs from subregions within the cortex. Two-tailed t-test, t = 3.38, * P < .05.

(*B*) Representative images of inputs from anterior cortical regions. D1-MSNs receive proportionally more input from medial orbitofrontal cortex (MO) than D2-MSNs.

(*C*) Quantitation of individual thalamic subregion inputs to D1- and D2-MSNs.

(*D*) Representative images of inputs from midline thalamic areas.
(*E*) Quantitation of inputs from amygdala subregions. Inset depicts percentage of all central amygdala inputs that localize to subdivisions within central amygdala (CeA) and representative image.
(F) Representative images of amygdala inputs to D1- and D2-MSNs.
Abbreviations: 3V, 3rd ventricle; LO, lateral orbitofrontal cortex; VO, ventral orbitofrontal cortex; PrL: prelimbic cortex; IL, infralimbic cortex; CM, central medial thalamic nucleus; Re, nucleus reuniens; Rh, rhomboid thalamic nucleus; MD, mediodorsal thalamic nucleus; Pf, parafascicular nucleus; EAM, extended amydala; CeC, capsular nucleus of CeA; CeM, medial nucleus of CeA; CeL, lateral nucleus of CeA. All scale bars: 250 μm.

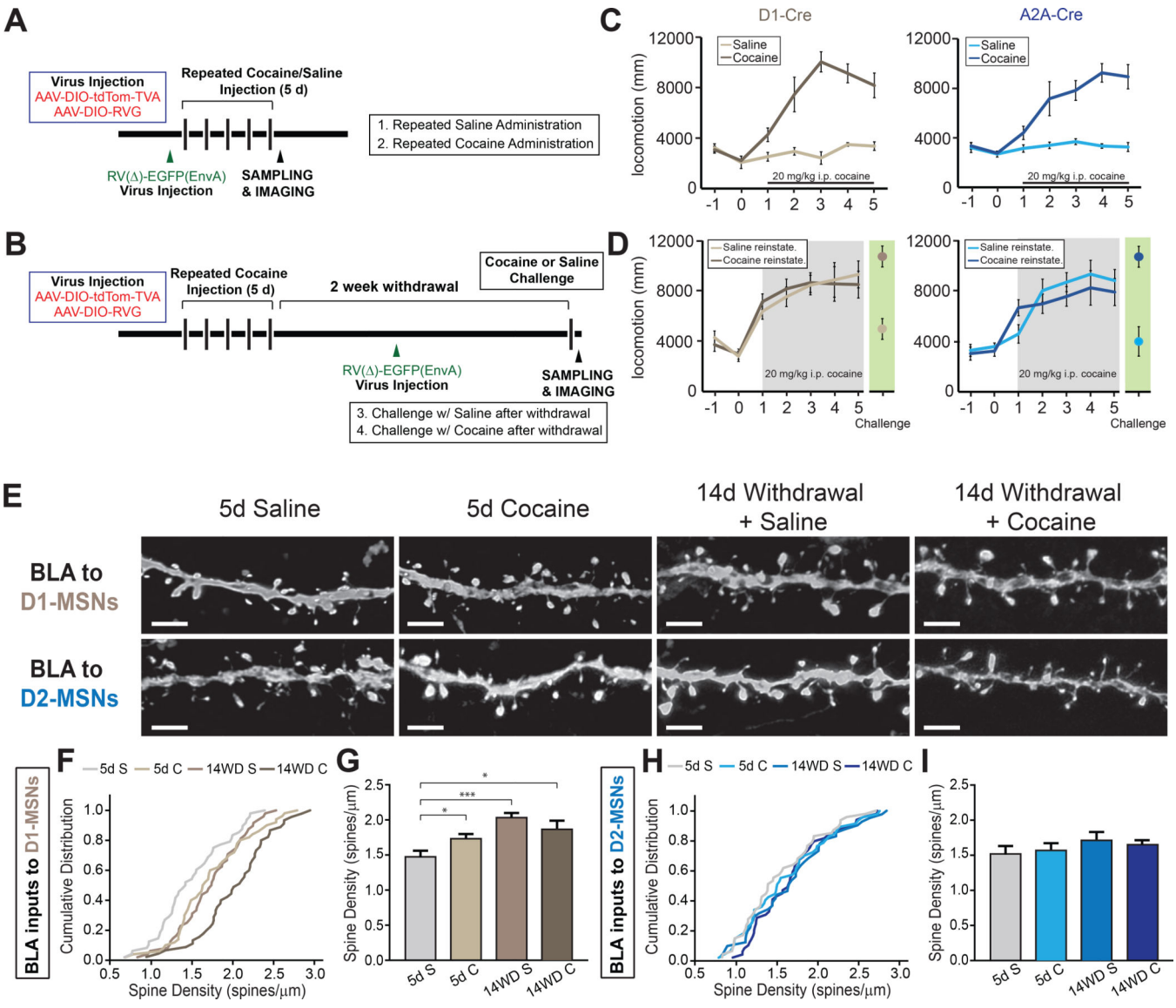

Figure 3.

Stage- and cell-type specific structural plasticity in basolateral amygdala (BLA) inputs to nucleus accumbens (NAc)

(*A* and *B*) Experimental timeline of viral injections and cocaine/saline administrations for 5 day administration group (*A*) and 5 day cocaine with 2 week withdrawal followed by either saline or cocaine reinstatement injection (*B*).

(*C* and D) Both genotypes exhibit locomotor sensitization with successive injections of cocaine (*C*) that persists after 2 weeks withdrawal with a cocaine, but not saline, reinstatement shot (*D*).

(*E*) Representative confocal images of dendritic spines of BLA neurons projecting to D1- and D2-receptor expressing medium spiny neurons (D1-MSNs, D2-MSNs, respectively) in NAc at separate stages of cocaine administration. Scale: 1 µm.

(*F*) Cumulative distribution plot of spine density of all dendrites imaged in BLA projecting to D1-MSNs. n = 48, 50, 45, 48 dendrites for 5d S (5 mice), 5d C (5 mice), 14WD S (6

mice), 14WD C (6 mice) groups, respectively. $p < .05$ for 5d S – 5d C and 5d S – 14WD C. $p < .001$ for 5d S – 14WD S; K-S test.

(*G*) Average spine densities at separate stages of cocaine administration in BLA dendrites projecting to D1-MSNs. K-S test, dendrites sampled as in (*F*).

(*H*) Cumulative distribution plot of spine density of all dendrites imaged in BLA projecting to D2-MSNs. n = 47, 47, 35, 44 dendrites for 5d S (4 mice), 5d C (5 mice), 14WD S (5 mice), 14WD C (6 mice), respectively.

(*I*) Average spine densities at separate stages of cocaine administration in D2-MSN projecting BLA neuronal dendrites. K-S test, dendrites sampled as in (*H*).

All data in (*G* and *I*) presented as mean ± SEM. Abbreviations: 5d S, 5 day acute saline; 5d C, 5 day acute cocaine; 14WD S, 14 day withdrawal saline reinstatement; 14WD C, 14 day withdrawal cocaine reinstatement. K-S test * $P < .05$, *** $P < .001$.

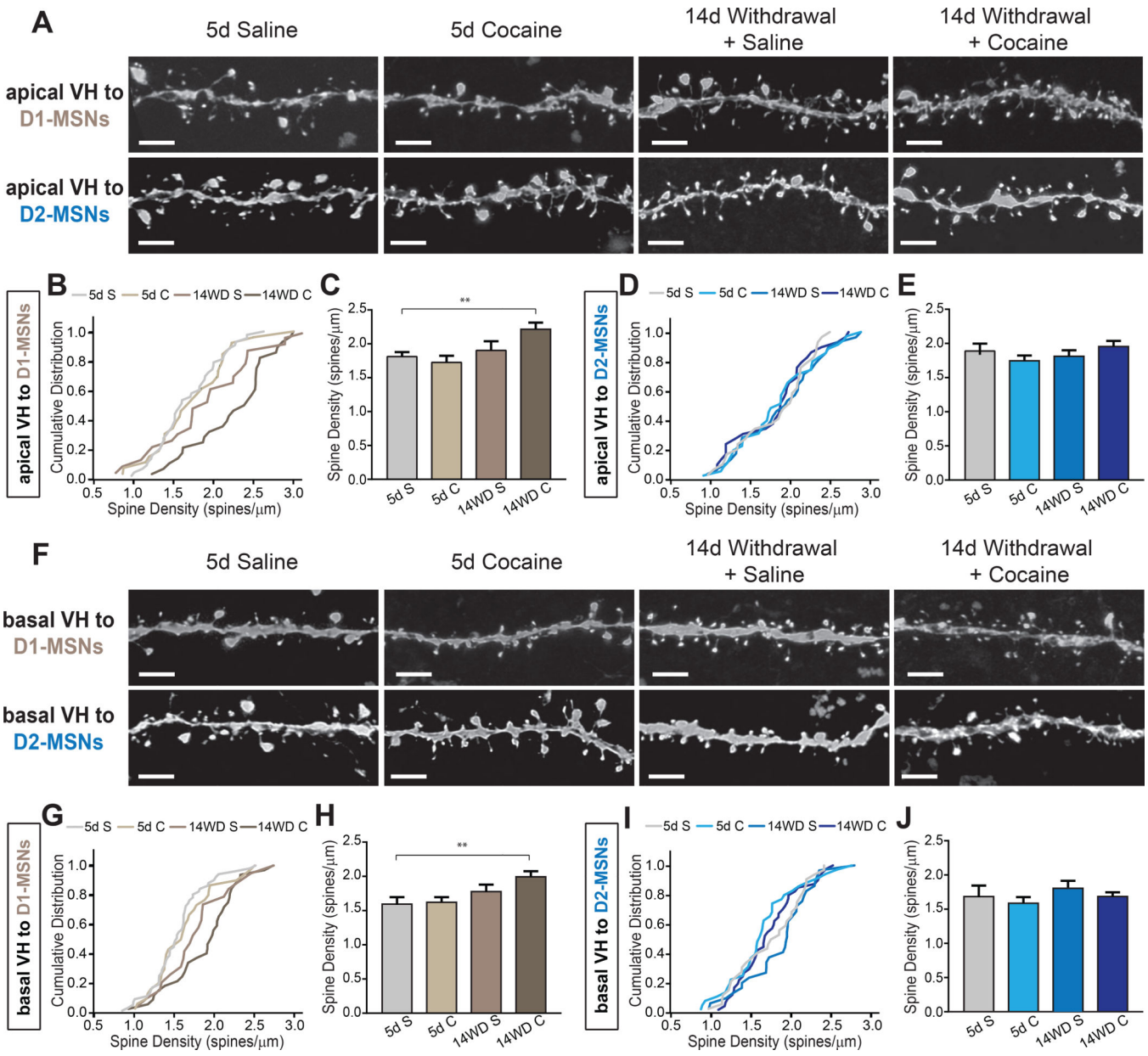

Figure 4.

Ventral hippocampal (vHPC) neurons projecting to D1-receptor expressing medium spiny neurons (D1-MSNs) exhibit increased dendrite spine density after withdrawal

(*A*) Representative images of apical dendritic spines in vHPC neurons projecting to NAc D1- and D2-receptor expressing MSNs (D2-MSNs) at different stages of cocaine administration. Scale: 1 μm.

(*B*) Cumulative distribution plots of apical vHPC dendrite density projecting to D1-MSNs. n = 37, 26, 25, 28 for 5d S (5 mice), 5d C (5 mice), 14WD S (5 mice), 14WD C (5 mice), respectively. $p < 0.01$ 5d S – 14WD C; Kolmogorov-Smirnov (K-S) test.

(*C*) Average spine densities of apical vHPC dendrites projecting to D1-MSNs at separate stages of cocaine administration. K-S test, dendrites sampled as in (*B*).

(*D*) Cumulative distribution plots of apical vHPC dendrite density projecting to D2-MSNs. n = 27, 33, 26, 25 for 5d S (4 mice), 5d C (5 mice), 14WD S (5 mice), and 14WD C (4 mice), respectively.
(*E*) Average spine densities of apical vHPC dendrites projecting to D2-MSNs at separate stages of cocaine administration. K-S test, dendrites sampled as in (*D*).
(*F*) Representative images of basal dendritic spines in vHPC neurons projecting to NAc D1- and D2-MSNs at different stages of cocaine administration. Scale: 1 μm.
(*G*) Cumulative distribution plots of basal vHPC dendrite density projecting to D1-MSNs. n = 46, 30, 20, 32 dendrites for 5d S (5 mice), 5d C (4 mice), 14WD S (4 mice), 14WD C (5 mice), respectively. $p < 0.001$ 5d S – 14WD C; K-S test.
(*H*) Average spine densities of basal vHPC dendrites projecting to D1-MSNs at separate stages of cocaine administration. K-S test, dendrites sampled as in (*G*).
(*I*) Cumulative distribution plots of basal vHPC dendrite density projecting to D2-MSNs. n = 29, 35, 25, 30 dendrites for 5d S (4 mice), 5d C (5 mice), 14WD S (4 mice), and 14WD C (5 mice), respectively.
(*J*) Average spine densities of basal vHPC dendrites projecting to D2-MSNs at separate stages of cocaine administration. K-S test, dendrites sampled as in (*I*).
Data in (*C, E, H, J*) presented as mean ± SEM. Abbreviations: 5d S, 5 day acute saline; 5d C, 5 day acute cocaine; 14WD S, 14 day withdrawal saline reinstatement; 14WD C, 14 day withdrawal cocaine reinstatement. K-S test ** $P < .01$.

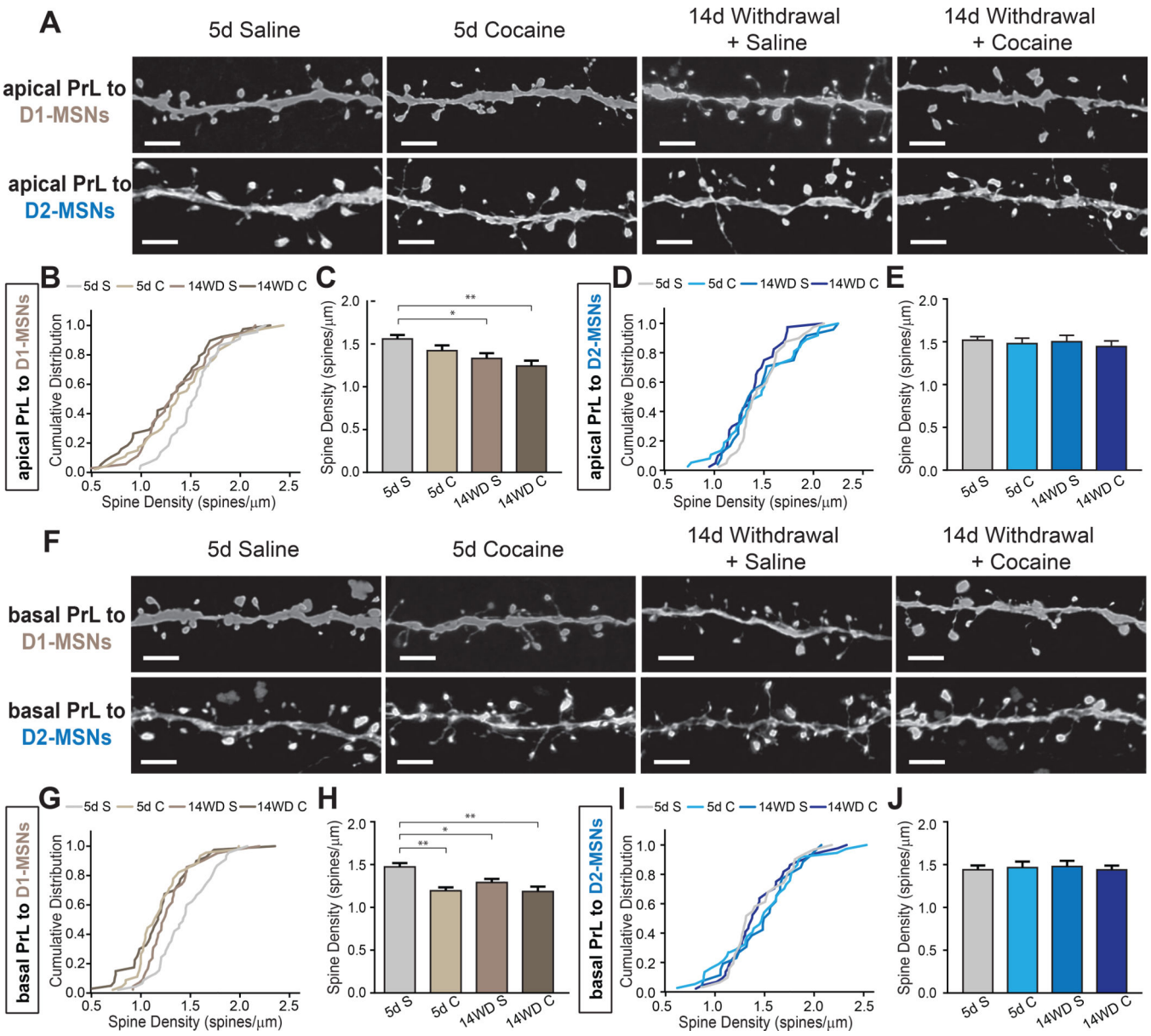

Figure 5.

Dendritic spine density of prelimbic cortex subregion (PrL) of medial prefrontal cortical (mPFC) neurons projecting to D1-receptor expressing, but not D2-receptor expressing medium spiny neurons (D1-MSN, D2-MSN, respectively) decrease after 14 day withdrawal.

(*A*) Representative confocal images of PrL neuronal apical dendrites and spines projecting to D1- and D2-MSNs. Scale: 1 μm

(*B*) Cumulative distribute plots of individual apical PrL dendrites projecting to D1-MSNs at different stages of cocaine administration. n = 44, 47, 36, 38 dendrites from 5d S (5 mice), 5d C (5 mice), 14WD S (5 mice), 14WD C (6 mice), respectively. $p < .05$ for 5d S – 14WD S, 5d S – 14WD C; Kolmogorov-Smirnov (K-S) test.

(*C*) Average spine densities of apical dendrites for D1-MSN projecting PrL neurons. K-S test, dendrites sampled as in (*B*).

(*D*) Cumulative distribute plots of individual apical PrL dendrites projecting to D2-MSNs at different stages of cocaine administration. n = 40 (5 mice), 37 (5 mice), 25 (4 mice), 40 (5 mice) dendrites for respective groups.

(*E*) Average spine densities of apical dendrites for D2-MSN projecting PrL neurons. K-S test, dendrites sampled as in (*D*).

(*F*) Representative confocal images of PrL neuronal basal dendrites and spines projecting to D1- and D2-MSNs. Scale: 1 μm.

(*G*) Cumulative distribute plots of individual D1-MSN projecting basal PrL dendrites at different stages of cocaine administration. n = 45, 45, 42, 40 dendrites from 5d S (5 mice), 5d C (5 mice), 14WD S (5 mice), 14WD C (6 mice), respectively. $P < .001$ for 5d S – 5d C, 5d S – 14WD C; $p < .05$ 5d S – 14WD S; all tested on K-S test.

(*H*) Average spine densities of basal dendrites for D1-MSN projecting PrL neurons. K-S test, dendrites sampled as in (*G*).

(*I*) Cumulative distribute plots of individual D2-MSN projecting basal PrL dendrites at different stages of cocaine administration. n = 30 (4 mice), 37 (5 mice), 26 (4 mice), 44 (5 mice) dendrites for respective groups.

(*J*) Average spine densities of basal dendrites for D2-MSN projecting PrL neurons. K-S test, dendrites sampled as in (*I*).

Data in *(C, E, H, J)* presented as mean ± SEM. Abbreviations: 5d S, 5 day acute saline; 5d C, 5 day acute cocaine; 14WD S, 14 day withdrawal saline reinstatement; 14WD C, 14 day withdrawal cocaine reinstatement. K-S test * $P < .05$, ** $P < .01$.

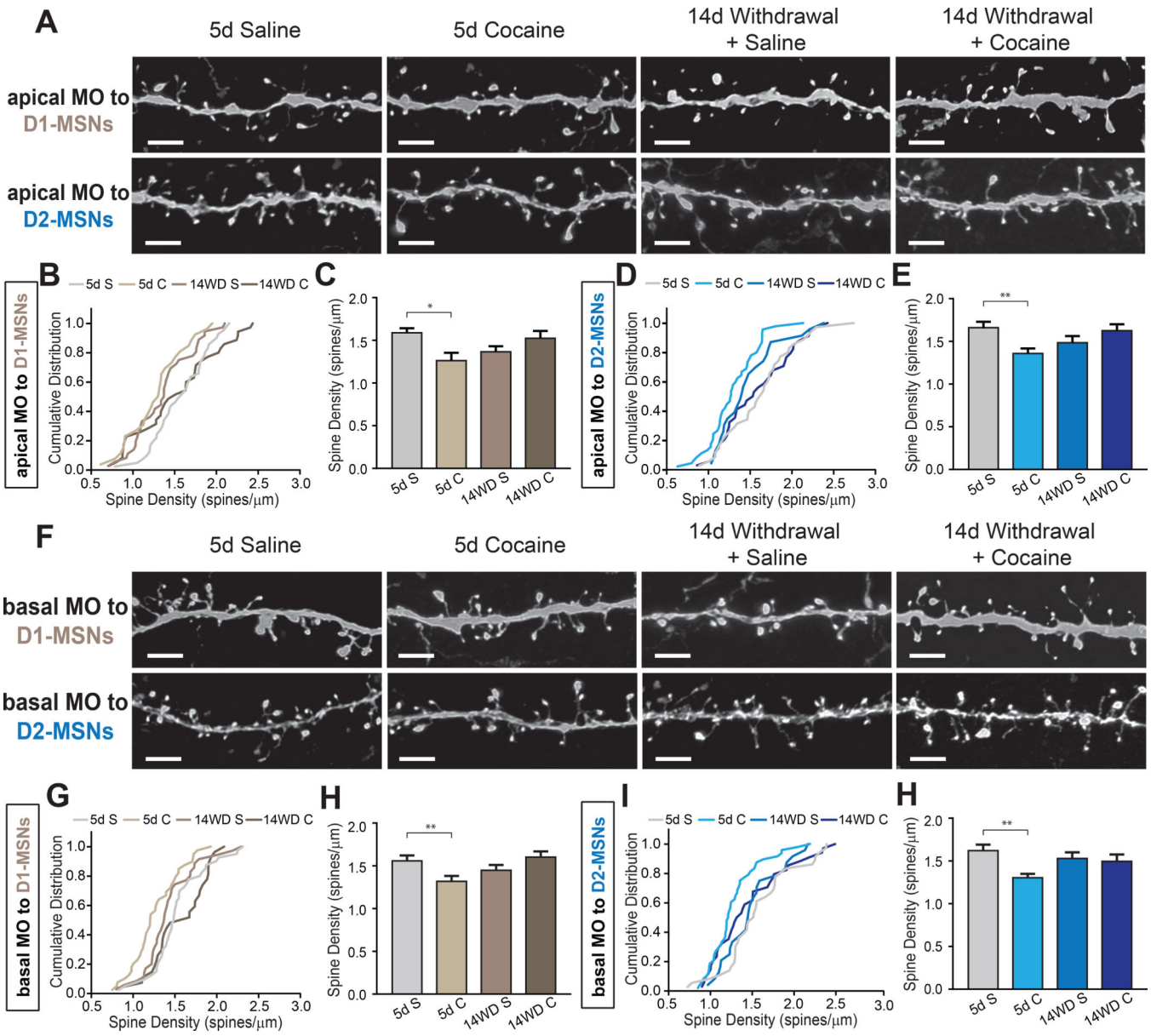

Figure 6.

Dendrites of medial orbitofrontal cortical (MO) neurons non-discriminately decrease spine density after 5 day cocaine treatment.

(*A*) Representative images of apical dendrites of MO neurons projecting to either D1- or D2-receptor expressing medium spiny neurons (D1-MSNs, D2-MSNs, respectively) in nucleus accumbens (NAc). Scale: 1 μm.

(*B*) Cumulative distribute plot of individual apical MO dendrites projecting to D1-MSNs at different stages of cocaine administration. n = 41, 26, 36, 35 dendrites for 5d S (5 mice), 5d C (5 mice), 14WD S (6 mice), 14WD C (5 mice), respectively. $P < .001$ for 5d S – 5d C, 5d S – 14WD C; $p < .05$ 5d S – 14WD S; all tested on K-S test.

(*C*) Average spine densities of apical dendrites for D1-MSN projecting MO neurons. K-S test, dendrites sampled as in (*B*).

(*D*) Cumulative distribute plot of individual apical MO dendrites projecting to D2-MSNs at different stages of cocaine administration. n = 35, 45, 23, 34 dendrites for 5d S (4 mice), 5d C (5 mice), 14WD S (4 mice), 14WD C (5 mice), respectively. P < .05 for 5d S – 5d C; K-S test.

(*E*) Average spine densities of apical dendrites for D2-MSN projecting MO neurons. K-S test, dendrites sampled as in (*D*).

(*F*) Representative images of apical dendrites of MO neurons projecting to either D1- or D2-MSNs in NAc. Scale: 1 μm.

(*G*) Cumulative distribute plots of individual basal MO dendrites projecting to D1-MSNs at different stages of cocaine administration. n = 40, 39, 35, 27 dendrites for 5d S (5 mice), 5d C (4 mice), 14WD S (5 mice), 14WD C (5 mice), respectively. P < .05 for 5d S – 5d C; K-S test.

(*H*) Average spine densities of basal dendrites for D1-MSN projecting MO neurons. K-S test, dendrites sampled as in (*G*).

(*I*) Cumulative distribute plots of individual basal MO dendrites projecting to D2-MSNs at different stages of cocaine administration. N = 36, 48, 24, 34 dendrites for 5d S (4 mice), 5d C (5 mice), 14WD S (5 mice), 14WD C (5 mice), respectively. P < .05 for 5d S – 5d C; K-S test.

(*H*) Average spine densities of apical dendrites for D2-MSN projecting MO neurons. K-S test, dendrites sampled as in (*I*).

Data in *(C, E, H, J)* presented as mean ± SEM. Abbreviations: 5d S, 5 day acute saline; 5d C, 5 day acute cocaine; 14WD S, 14 day withdrawal saline reinstatement; 14WD C, 14 day withdrawal cocaine reinstatement. K-S test * P < .05, ** P < .01.